

## STRUCTURAL PROPERTIES OF Al-DOPED ZnO FILMS

 Sirajidin S. Zainabidinov<sup>a</sup>,  Shakhriyor Kh. Yulchiev<sup>b</sup>,  Akramjon Y. Boboev<sup>a,c</sup>,  
 Bakhtiyor D. Gulomov<sup>d</sup>,  Nuritdin Y. Yunusaliyev<sup>a</sup>

<sup>a</sup>Andijan state university named after Z.M. Babur, Andijan, Uzbekistan

<sup>b</sup>Andijan state pedagogical institute, Andijan, Uzbekistan

<sup>c</sup>Institute of Semiconductor Physics and Microelectronics at the National University of Uzbekistan,  
20 Yangi Almazar st., Tashkent, 100057, Uzbekistan

<sup>d</sup>Andijan Machine-Building Institute, Andijan, 170119, Uzbekistan

\*Corresponding Author e-mail: [aboboevscp@gmail.com](mailto:aboboevscp@gmail.com)

Received June 30, 2024; revised July 25, 2024; accepted August 5, 2024

In this study, the results of the investigation of the influence of Al atoms on the structural characteristics of ZnO films obtained by the sol-gel method are presented. It has been determined that the glass substrates consist of subcrystallites with dimensions of 28.6 nm, having cubic unit cells with lattice parameters  $a = 0.3336$  nm, and their surfaces belong to the crystallographic orientation (111). It has been identified that the grown thin ZnO films consist of subcrystallites with dimensions of 39.5 nm, having a wurtzite structure with lattice parameters  $a = b = 0.3265$  nm and  $c = 0.5212$  nm, respectively. It has been determined that at the boundaries of the division of these subcrystallites, polycrystalline regions with sizes of 12.6 nm, 28.3 nm, 30 nm, and 33 nm are formed. Additionally, nanocrystallites with sizes of 56.8 nm self-assemble on the surface areas of the deposited films. The increase in the values of the “c” axis of the hexagonal crystal lattice of ZnO films by 0.0009 nm when doping Al atoms from 1% to 5% is explained by the shift of the main structural line (002) at small angles ( $\Delta\theta=0.12^\circ$ ). It has been established that nanocrystallites with lattice parameters  $a_n = 0.5791$  nm, belonging to the spatial group  $Fd\bar{3}m$ , self-assemble on the surface areas of ZnO:Al films. The curve due to the presence of a monoenergetic level of fast surface states at the heterojunction.

**Keywords:** Borosilicate glass; Sol-gel method; Metal oxide; ZnO thin film; X-ray diffraction; Subcrystallite; Nanocrystal

**PACS:** 78.30.Am

### INTRODUCTION

Currently, due to the rapid development of optoelectronics and nanoelectronics, thin films of ZnO with their sufficiently wide band gap (3.37 eV) are of great interest to both researchers and manufacturers of optoelectronic equipment. In addition to the simplicity and well-studied synthesis technology, the relatively low prices of the raw materials allow for the wide application of ZnO in production. Research shows that the unique physical and chemical properties of thin layers of ZnO open up the possibility of their wide application in many micro and nanoelectronic devices such as gas sensors, optical and magnetic storage devices, solar cells, piezoelectric conductors, photodiodes, photodetectors, etc. [1,2].

In addition, the possibility of controlling the electrical and photoconductivity of ZnO thin films by doping with various impurity atoms is attractive. Films of ZnO were grown using centrifugation, magnetron sputtering, and spray pyrolysis methods in works [3-5], and the optimal doping conditions of Al impurity atoms in these films were determined, as well as their piezoelectric and optoelectronic properties were studied. However, reliable results on the influence of different concentrations of impurity atoms on the structural properties of ZnO films are still lacking, which is an important issue for the stable functioning of devices. Therefore, this study presents the results of investigating the influence of Al impurity atoms on the structural characteristics of ZnO films obtained by the sol-gel method using the immersion technique.

### MATERIALS AND METHODS

To prepare the required sol-gel solution, zinc acetate ( $Zn(CH_3COO)_2 \cdot 2H_2O$ ) was used as a precursor, isopropyl alcohol ( $CH_3CH(OH)CH_3$ ) as a solvent, diethylamine ( $C_4H_{11}N$ ) as a stabilizer, and aluminum nitrate ( $Al(NO_3)_3 \cdot 9H_2O$ ) as an additive. Zinc acetate (3.23 grams) and aluminum nitrate (0.047-0.265 grams), dissolved in isopropyl alcohol (100 ml), were slowly added dropwise with diethylamine (0.33 ml) to increase solubility. The mixture was stirred using a magnetic stirrer at 60°C and a speed of 1500 rpm until the solution became clear. To convert the prepared sol-gel solution into a gel, it was incubated in a special cabinet at room temperature for 168 to 240 hours. In the deposition setup, the optimal repeatability of processes was about 20 times when growing thin layers of ZnO, both pure and doped with aluminum atoms (from 1% to 5%). To remove any undissolved gel from the surface of the grown films, they were subjected to thermal treatment at 500°C for 10 minutes in a drying oven. X-ray diffraction studies of the grown films were conducted using an XRD-6100 X-ray diffractometer [6]. To determine the resistivity, concentration and the mobility of the majority charge carriers in the grown films, the Van der Pauw method was used on a HMS-7000 Hall effect measurement unit [7].

## RESULTS AND DISCUSSION

Figure 1 shows the X-ray diffraction pattern of the borosilicate glass substrates used in our study. The diffraction pattern at a scattering angle of  $2\theta = 47.1^\circ$  with  $d/n = 0.1926$  nm exhibits a structural reflex with a crystallographic orientation of (111). This indicates that the majority of atoms in the substrate are arranged in a crystallographic orientation of (111) and its surface also belongs to this plane. Furthermore, based on the experimental values of the structural reflection (111), the lattice parameter ( $a_s$ ) of the substrate was determined to be 0.3336 nm using the Nelson-Riley extrapolation function [8-10]. Based on the width of the crystallographic orientation (111), the size of the blocks (subcrystallites) was determined to be 28.6 nm. The fact that the structural reflection (111) has a width of  $5.5 \times 10^{-3}$  radians and a high intensity ( $\sim 104$  imp s $^{-1}$ ) indicates a high degree of crystallinity of the borosilicate substrate [11]. Furthermore, the diffraction pattern showed structural reflections corresponding to crystallographic directions (200) at an angle of  $2\theta = 55.031^\circ$  with  $d/n = 0.1668$  nm, (210) at an angle of  $2\theta = 62.13^\circ$  with  $d/n = 0.1492$  nm, and (211) at an angle of  $2\theta = 68.57^\circ$  with  $d/n = 0.1362$  nm. Analysis of these experimental results showed that the sizes of the corresponding crystallites, according to expression (3), were approximately 20 nm. The Observation of such structural lines suggests the presence of polycrystalline regions at the boundaries of subcrystallites of the borosilicate substrate [12]. The observed structural reflection corresponding to the crystallographic direction (110) at a scattering angle of  $2\theta = 38.1^\circ$  with  $d$ -spacing  $d/n = 0.2359$  nm indicates the presence of nanopores sized 81.5 nm on the substrate surface [13]. Additionally, at a low angle of approximately  $2\theta \approx 15^\circ$ , the X-ray diffraction pattern shows broad diffuse reflection caused by structural fragments of  $\text{SiO}_x$  on the surface layers, which contain unsaturated bonds of silicon and oxygen atoms. The half-width ( $\beta = 1.25 \times 10^{-1}$  rad) of this reflection indicates small sizes of the  $\text{SiO}_x$  structural fragment and the absence of long-range order in their arrangement. Thus, these  $\text{SiO}_x$  structural fragments represent atomic clusters rather than nanocrystallites, with characteristic sizes of approximately 1.2 nm [14].

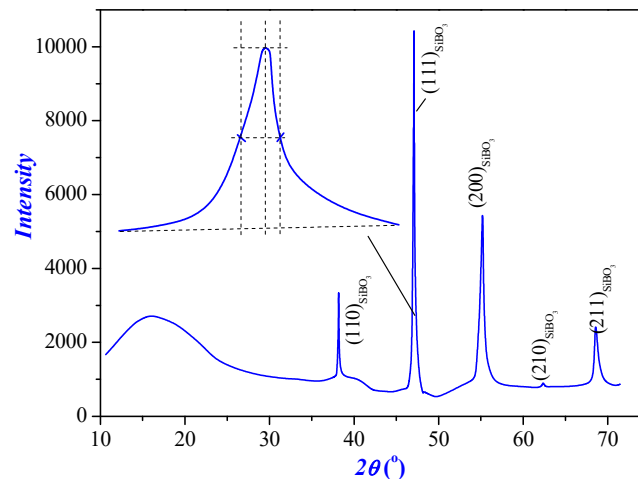


Figure 1. X-ray diffraction pattern of borosilicate glass

In Figure 2 (black curve), the X-ray diffraction pattern of ZnO films is shown, which significantly differs from the substrate's diffraction pattern.

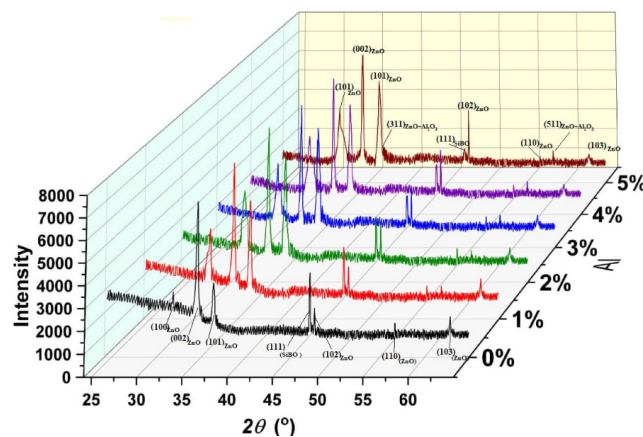


Figure 2. X-ray diffraction patterns of (a) undoped and (b-1%, c-2%, d-3%, e-4%, and f-5%) Al doped ZnO films.

It can be observed that at low-angle scattering, diffuse reflection with three highly intensive selective structural reflexes is present, belonging to the crystallographic orientation (100) at a scattering angle of  $2\theta = 31.42^\circ$  with  $d/n = 0.2774$  nm, (002) at an angle of  $2\theta = 34.48^\circ$  with  $d/n = 0.2581$  nm, and (101) at a scattering angle of  $2\theta = 36.34^\circ$

with  $d/n = 0.249$  nm. Among these observed reflexes, the structural line corresponding to the crystallographic direction (002) has the highest intensity ( $\sim 104 \text{ imp}\cdot\text{c}^{-1}$ ) (Figure 2, black curve). Based on these experimental values, the calculated full width at half maximum of this reflection was  $3.9 \times 10^{-3}$  radians, indicating a relatively high degree of crystallinity of the grown film. Upon analysis of the experimental results of this reflection, the constant of the crystal lattice has been determined, which are equal to  $a = b = 0.3265$  nm and  $c = 0.5212$  nm, respectively. This, in turn, allows to determine that the ZnO layers have a wurtzite structure, belonging to the hexagonal crystal lattice of the spatial group  $C6/mmc$ , which is provided by the alternate placement of zinc and oxygen in the elementary cell of the crystal lattice [9]. Using expression (3), the sizes of subcrystallites in unalloyed ZnO films were determined from the experimental values of the (002) reflection shape, which were approximately 39.5 nm. Additionally, double structural reflections belonging to the crystallographic orientations (111) and (102) are observed on the X-ray diffraction pattern of the grown films in the scattering angle range of  $47.0^\circ$  to  $47.48^\circ$ , corresponding to the substrate and ZnO film, respectively (Fig. 3, black curve). The structural line (111) belongs to the borosilicate substrate, located deeper in the ZnO film with a thickness of  $1 \mu\text{m}$ , thus appearing due to the rays returning from the substrate surface.

In addition to the structural lines observed in the X-ray diffraction pattern, which belong to the crystallographic orientations (110) at an angle of  $2\theta = 56.67^\circ$  with  $d/n = 0.1630$  nm, (103) at an angle of  $2\theta = 62.93^\circ$  with  $d/n = 0.1481$  nm, (200) at an angle of  $2\theta = 66.37^\circ$  with  $d/n = 0.1398$  nm, (212) at an angle of  $2\theta = 66.52^\circ$  with  $d/n = 0.1376$  nm, and (201) at an angle of  $2\theta = 69.17^\circ$  with  $d/n = 0.1327$  nm. This, in turn, indicates that polycrystalline regions of 12.6 nm, 28.3 nm, 30 nm, and 33 nm in size, with different shapes, as well as nanocrystallites of 56.8 nm in the near-surface layers of grown ZnO films, self-assemble at the boundaries of subcrystallites.

In Figure 2 (curves red, green, blue, violet, and brown), X-ray diffraction patterns of doped Al (from 1% to 5%) thin films of ZnO are presented, which significantly differ from the X-ray diffraction pattern of pure ZnO film. It can be observed that their elastic background level of diffuse reflection, observed at low-angle scattering, decreases with an increase in the amount of dopant atoms. This indicates that with an increase in the amount of Al dopant atoms in the grown films, the uneven distribution of oxygen from the main background impurities along the crystal lattice decreases [4]. Additionally, besides this diffuse reflection, reflections corresponding to the crystallographic orientations (100) are observed at an angular scattering angle of  $2\theta = 31.7^\circ$  with  $d$ -spacing  $d/n = 0.2774$  nm, and (101) at an angular scattering angle of  $2\theta = 36.34^\circ$  with  $d$ -spacing  $d/n = 0.249$  nm, shifted towards smaller angles by  $\Delta\theta = 0.06^\circ$  and  $\Delta\theta = 0.08^\circ$ , respectively. Simultaneously, in the X-ray diffraction patterns of the film with aluminum alloying atoms up to 2%, their intensities increase to 28.1% for the structural line (100) and 37.8% for the structural line (101). However, with alloying atoms above 2%, their intensities decrease by 4.29% and 1.6%, respectively. This indicates that instead of the structural lines (100) and (101), new reflections appear belonging to the crystallographic directions (220) and (311) of the ZnO and  $\text{Al}_2\text{O}_3$  compounds [15].

From Figure 3, it can be seen that the main structural reflex belonging to the crystallographic direction (002) on the X-ray diffraction pattern is shifted towards small angles (from  $2\theta = 34.44^\circ$  to  $2\theta = 34.32^\circ$ ), i.e. by  $\Delta\theta = 0.12^\circ$  with an increase in the number of Al alloying atoms.

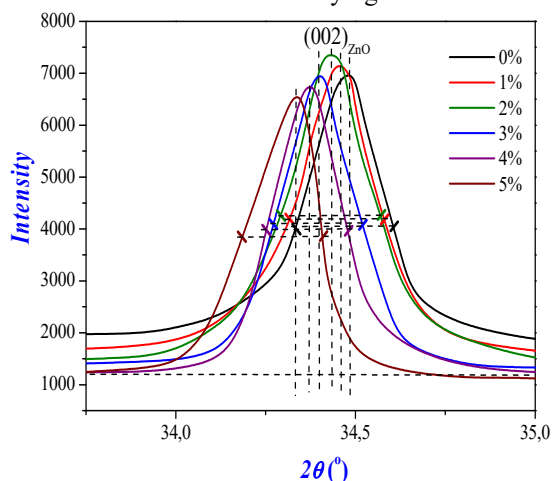


Figure 3. Reflex shape (002) of X-ray diffraction patterns of undoped and Al doped (from 1% to 5%) ZnO films

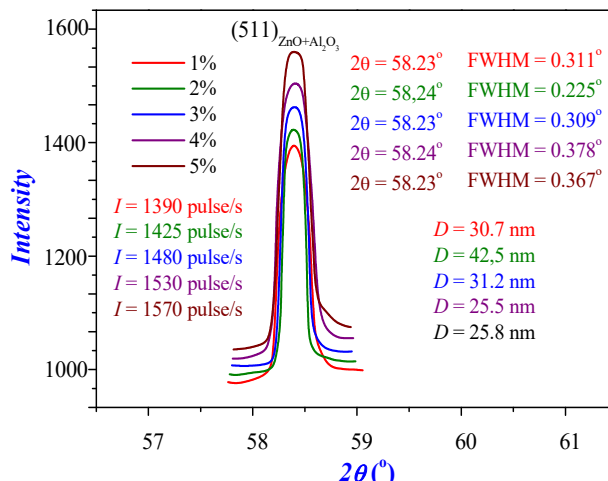


Figure 4. The forms of reflexes (511) of X-ray diffraction patterns of undoped and Al doped (from 1% to 5%) ZnO films

Their intensity increased to 5.2% for samples alloyed with Al up to 2% and decreased to 6.3% for samples with an Al content exceeding 2% (Figure 3, curves red, green, blue, violet, and brown). Analyzing the experimental results of these reflections using expression (4), it was established that the lattice parameter of the crystal at room temperature for films with Al alloying atoms is  $a = b = 0.3265$  nm and  $c = 0.5219$  nm, while the axes of the hexagonal crystal lattice increase by a small amount ( $\Delta c = 0.0009$  nm). This indicates that in the crystal lattice of the film,  $\text{Al}^{+3}$  ions are replaced by  $\text{Zn}^{+2}$  ions [15]. When determining the half-width ( $\beta$ ) of these reflexes according to expression (2), they initially increased (doping with Al atoms up to 3%), and then decreased (doping with Al atoms more than 3%). This allows

determining the sizes of subcrystallites according to expression (3), which initially decreased (when doping with Al atoms up to 2%) ( $D_{0\%Al:ZnO} = 39.5$  nm,  $D_{1\%Al:ZnO} = 37.9$  nm, and  $D_{2\%Al:ZnO} = 34.1$  nm), then increased when doping with Al atoms more than 2% ( $D_{3\%Al:ZnO} = 34.4$  nm,  $D_{4\%Al:ZnO} = 35.2$  nm, and  $D_{5\%Al:ZnO} = 35.8$  nm). Based on the experimental values of these reflections, it can be concluded that doping ZnO with Al atoms up to 2% leads to an increase in the perfection of the crystal lattice of the films, while an increase in Al atoms more than 2% leads to their decrease [15]. Furthermore, the structural reflexes on the ZnO X-ray diffraction pattern increase when doped with Al atoms up to 2% and decrease with further increase in their concentration beyond 2%. Consequently, aluminum atoms incorporated into the ZnO crystal lattice up to 2% combine with oxygen, which acts as atoms of an uncontrolled background level, resulting in the organization of clusters corresponding to ZnO and  $Al_2O_3$  compounds at an angle of  $2\theta = 58.4^\circ$  with  $d/n = 0.15740$  nm, leading to the emergence of new structural lines. Conversely, with an increase in doping of Al atoms above 2% in the crystal lattice, small microstrains are formed in the film. The structural lines corresponding to crystallographic orientations (110), (103), (200), (212), and (201) on the X-ray diffraction pattern change disproportionately with the increase in the number of added Al atoms. However, the sizes of these crystallites have partially decreased, forming various polycrystalline regions ranging in size from 11 nm to 30 nm.

As a result of the mutual substitution of ZnO and  $Al_2O_3$  compounds, structural lines belonging to crystallographic directions (311) were observed on the X-ray diffraction pattern of ZnO films doped with Al atoms at a scattering angle of  $2\theta = 58.23^\circ$  with d-spacing of 0.1574 nm (Fig. 4). Based on the experimental values of these structural lines using equations (1), (2), and (3), parameters of their lattices, full width at half maximum ( $\beta$ ), and sizes of crystallites were determined.

The sizes of crystallites and the values of  $\beta$  varied with increasing amounts of Al dopant atoms (as a percentage: 1%, 2%, 3%, 4%, and 5%), specifically 31 nm, 42 nm, 31 nm, 25 nm, and 26 nm. Phase analysis of the experimental results of these reflections indicates that they originated from a phase different from the main phase, specifically from a phase with a cubic elementary cell belonging to space group  $Fd3m$  and with a lattice constant of 0.5791 nm. This, in turn, indicates the formation of distinct crystallographic nanocrystallites of a specific size and orientation in the (511) order in near-surface defect-prone regions of ZnO films doped with Al (from 1% to 5%).

Additionally, using the results of X-ray structural studies (relative analysis of structural reflections [16]), we determined the chemical composition of the grown films, and their calculated data are presented in Table 1.

**Table 1.** Proportions of grown film components

Components	Films	ZnO:Al				
	ZnO					
Zn, at%	49.89	29.93	29.47	28.17	27.55	26.52
O, at%	50.11	68.78	68.61	68.49	68.36	68.25
Al, at%	-	1.29	1.92	3.34	4.09	5.23

In accordance with the information provided, the proportion of Al atoms in relation to the total number of atoms in the films was 1.29%, 1.92%, 3.34%, 4.09%, and 5.22%, respectively.

## CONCLUSION

Based on the conducted experimental research and analysis of the obtained results, the following conclusions can be drawn:

It has been established that the surface of the borosilicate substrate has a crystallographic orientation of (111) and consists of subcrystallites with a size of 28.6 nm, having a lattice constant as  $= 0.3336$  nm, belonging to the space group  $Pm3m$ . Additionally, the presence of polycrystalline regions approximately 20 nm in size at the boundaries between the subcrystallites of the substrate has been detected. Nanovoids with a size of  $\sim 81.5$  nm is observed in its near-surface area, as well as structural fragments of  $SiO_x$  with dimensions of  $\sim 1.2$  nm exhibiting amorphous properties.

It has been established that the surface of the grown ZnO films belongs to the crystallographic direction (002) and consists of blocks with dimensions of 39.5 nm, exhibiting a hexagonal crystalline lattice structure of wurtzite with lattice periods  $a = b = 0.3265$  nm and  $c = 0.5212$  nm, belonging to space group  $C6/mmc$ . It has also been determined that within the volume and on the surface of the films, self-organized polycrystalline regions of sizes 12.6 nm, 28.3 nm, 30 nm, and 33 nm, as well as nanocrystallites with a size of 56.8 nm, are formed.

It has been identified that  $Al^{+3}$  ions replace  $Zn^{+2}$  ions in the crystalline lattice forming the ZnO film, leading to a slight increase in the c-axis of the hexagonal crystalline lattice ( $\Delta c = 0.0009$  nm), as determined by the slight shift of the main (002) crystallographic lines at small angles ( $\Delta\theta = 0.12^\circ$ ).

ZnO films with Al atom concentrations (from 1% to 5%) exhibit nanocrystallites with a lattice constant of 0.5791 nm, forming in near-surface areas as compounds of ZnO and  $Al_2O_3$ , belonging to the spatial group type  $Fd3m$ .

## Conflict of Interests

The authors declare that they have no conflict of interests

## Funding

The work was carried out using project funds allocated according to the order of the rector of Andijan State University dated February 7, 2024, No. 04-12.

ORCID

- ©Sirajidin S. Zainabidinov, <https://orcid.org/0000-0003-2943-5844>; ©Shakhriyor Kh. Yulchiev, <https://orcid.org/0009-0007-2576-4276>  
©Akramjon Y. Boboev, <https://orcid.org/0000-0002-3963-708X>; ©Bakhtiyor D. Gulomov, <https://orcid.org/0009-0005-8614-6311>  
©Nuritdin Y. Yunusaliyev, <https://orcid.org/0000-0003-3766-5420>

REFERENCES

- [1] S. Zainabidinov, S.I. Rembeza, E.S. Rembeza, Sh.Kh. Yulchiev, "Applied Solar Energy," Academic Journal, **55**(1), 5 (2019). <https://doi.org/10.3103/S0003701X19010146>
- [2] Kh. J. Mansurov, A.Y. Boboyev, and J.A. Urinboev, "X-ray structural and photoelectric properties of SnO<sub>2</sub>, ZnO, and Zn<sub>2</sub>SnO<sub>4</sub> metal oxide films," East European Journal of Physics. (2), 336-340 (2024). <https://doi.org/10.26565/2312-4334-2024-2-39>
- [3] M. Laurenti, S. Stassi, M. Lorenzoni, M. Fontana, G. Canavese, V. Cauda, and C.F. Pirri, "Evaluation of the piezoelectric properties and voltage generation of flexible zinc oxide thin films," Nanotechnology, **26**(21), 1 (2019) <https://doi.org/10.1088/0957-4484/26/21/215704>
- [4] K. Chongsri, and W. Pecharapa, "UV Photodetector Based On Al-Doped ZnO Nanocrystalline Sol-Gel Derived Thin Films" Energy Procedia, **56**, 554–559 (2014). <https://doi.org/10.1016/j.egypro.2014.07.192>
- [5] P. Koralli, S.F. Varol, G. Mousdis, D.E. Mouzakis, Z. Merdan, M. Kompitsas, "Chemosensors. Comparative Studies of Undoped/Al-Doped/In-Doped ZnO Transparent Conducting Oxide Thin Films in Optoelectronic Applications," Chemosensors, **10**(5), 162 (2022). <https://doi.org/10.3390/chemosensors10050162>
- [6] F.I. Alreshedi, and J.E. Krzanowski, "X-ray Diffraction Investigation of Stainless Steel—Nitrogen Thin Films Deposited Using Reactive Sputter Deposition," Coatings, **10**, 984 (2020). <https://doi.org/10.3390/coatings10100984>
- [7] S.Z. Zainabidinov, A.Y. Boboev, and N.Y. Yunusaliyev, "Effect of  $\gamma$ -irradiation on structure and electrophysical properties of S-doped ZnO films," East European Journal of Physics, (2), 321-326 (2024). <https://doi.org/10.26565/2312-4334-2024-2-37>
- [8] S. Zainabidinov, Sh. Yuldashev, A. Boboev, and N. Yunusaliyev, "X-ray diffraction and electron microscopic studies of the ZnO(S) metal oxide films obtained by the ultrasonic spray pyrolysis method," Herald of the Bauman Moscow State Technical University, Series Natural Sciences, **1**(112), 78-92 (2024). <https://doi.org/10.18698/1812-3368-2024-1-78-92>
- [9] S.Z. Zainabidinov, Sh.B. Utamuradova, and A.Y. Boboev, "Structural Peculiarities of the (ZnSe)<sub>1-x-y</sub>(Ge<sub>2</sub>)<sub>x</sub>(GaAs<sub>1- $\delta$</sub> Bi <sub>$\delta$</sub> )<sub>y</sub> Solid Solution with Various Nano-inclusions," Journal of Surface Investigation, Synchrotron and neutron techniques, 48-52 (2024). <https://doi.org/10.18698/1812-3368-2024-1-78-92>
- [10] V. Utyaganova, et al., "Controlling the porosity using exponential decay heat input regimes during electron beam wire-feed additive manufacturing of Al-Mg alloy," The International Journal of Advanced Manufacturing Technology, **108**, 2823–2838 (2020). <https://doi.org/10.1007/s00170-020-05539-9>
- [11] B. Parveena, M. Hassan, Z. Khalida, S. Riadz, and S. Naseem "Room-temperature ferromagnetism in Ni-doped TiO<sub>2</sub> diluted magnetic semiconductor thin films," Journal of Applied Research and Technology, JART, **15**(2), 132-139 (2017). <https://doi.org/10.1016/j.jart.2017.01.009>
- [12] L.S. Vasil'ev, I.L. Lomaev, and S.L. Lomaev, "On the Structure Of Segregations At Special Boundaries Of Polycrystalline Substitutional Alloys," Russian Physics Journal, **64**(10), 45-46 (2022). <https://doi.org/10.1007/s11182-022-02532-5>
- [13] M.F. Malek, M.H. Mamat, Z. Khusaimi, M.Z. Sahdan, M.Z. Musa, A.R. Zainun, A.B. Suriani, et al., "Sonicated sol-gel preparation of nanoparticulate ZnO thin films with various deposition speeds: The highly preferred c-axis (0 0 2) orientation enhances the final properties," Journal of Alloys and Compounds, **582**, 12-21(2014) <https://doi.org/10.1016/j.jallcom.2013.07.202>
- [14] V. Bratus, and V. Yukhimchuk, "Structural Transformations and Silicon Nanocrystallite Formation in SiO<sub>x</sub> Films," FTP, **35**(7), 854–860 (2001). <https://doi.org/10.63-7826/01/3507-21.00>
- [15] A. Ghazai, E. Salman, and Z. Jabbar, "Effect of Aluminum Doping on Zinc Oxide Thin Film Properties Synthesis by Spin Coating Method," American Scientific Research Journal for Engineering Technology, and Sciences (ASRJETS), **26**(3), 202-203 (2016).
- [16] G. Fetisov, "X-ray diffraction methods for structural diagnostics of materials: progress and achievements," Physics - Uspekhi **63**(1), 2-32 (2020). <https://doi.org/10.3367/ufne.2018.10.038435>

СТРУКТУРНІ ВЛАСТИВОСТІ ПЛІВОК ZnO, ЛЕГОВАНИХ Al

Сіражідін С. Зайнабідінов<sup>a</sup>, Шахрїйор Х. Юльчїєв<sup>b</sup>, Акрамжон Ю. Бобоев<sup>a,c</sup>,  
Бахтїйор Д. Гуломов<sup>d</sup>, Нурїтдїн Ю. Юнусалїєв<sup>a</sup>

<sup>a</sup>Андижанський державний університет імені З.М. Бабура, Андижан, Узбекистан

<sup>b</sup>Андижанський державний педагогічний інститут, Андижан, Узбекистан

<sup>c</sup>Інститут фізики напівпровідників та мікроелектроніки Національного університету Узбекистану, Ташкент, Узбекистан

<sup>d</sup>Андижанський машинобудівний інститут, Андижан, Узбекистан

У даній роботі наведено результати дослідження впливу атомів Al на структурні характеристики плівок ZnO, отриманих золь-гель методом. Встановлено, що скляні підкладки складаються з субкристалітів розміром 28,6 нм, які мають кубічні елементарні комірки з параметрами ґратки  $a = 0,3336$  нм, а їх поверхні належать до кристалографічної орієнтації (111). Встановлено, що вирощені тонкі плівки ZnO складаються з субкристалітів розміром 39,5 нм, які мають структуру вюрциту з параметрами решітки  $a = b = 0,3265$  нм і  $c = 0,5212$  нм відповідно. Встановлено, що на межах поділу цих субкристалітів утворюються полікристалічні області з розмірами 12,6 нм, 28,3 нм, 30 нм і 33 нм. Крім того, нанокристаліти розміром 56,8 нм самоорганізуються на поверхнях нанесених плівок. Збільшення значень осі «с» гексагональної кристалічної ґратки плівок ZnO на 0,0009 нм при легуванні атомів Al від 1% до 5% пояснюється зміщенням основної структурної лінії (002) на малі кути ( $\Delta\theta = 0,12^\circ$ ). Встановлено, що нанокристаліти з параметрами ґратки  $a_p = 0,5791$  нм, що належать до просторової групи Fd3m, самоорганізуються на ділянках поверхні плівок ZnO:Al. крива через наявність моноенергетичного рівня швидких поверхневих станів на гетеропереході.

**Ключові слова:** боросилікатне скло; золь-гель метод; оксид металу; тонка плівка ZnO; рентгенівська дифракція; субкристаліт; нанокристал